PCCP

Accepted Manuscript

ROYAL SOCIETY OF CHEMISTRY

www.rsc.org/pccp

First Observation of HO$^{\bullet}$ Reactivity in Water under High Energy Ions at Elevated Temperature

A. Balcerzyk[†#], *I. Boughattas*[#], *S. Pin*[†#], *E. Balanzat*[$], *and G. Baldacchino*[†#*]

† CEA Saclay, IRAMIS, SIS2M, LRad, Bât 546, PC 175, F-91191 Gif-sur-Yvette Cedex, France

[#] CNRS, SIS2M, UMR3299 CEA-CNRS, Bât 125, PC 9, F-91191 Gif-sur-Yvette Cedex, France

[$] CIMAP, GANIL UMR CEA-CNRS-ENSI Caen, BP5133, F-14070 Caen Cedex 5, France

ABSTRACT

This communication reports the first observation of the formation of $HO^{\bullet}$ produced under two different high energy ion beams, $^{18}O^{8+}$ and $^{36}Ar^{18+}$ having Linear Energy Transfers (LET) of 65 and 350 eV·nm^{-1} respectively, at temperatures up to 411 K. Both scavenging with various concentrations of SCN^- and heavy-ion pulse radiolysis methods are used with an original temperature and pressure regulated optical cell. Deconvolution of kinetics is used to analyze the evolution of $HO^{\bullet}$ track segment yields as a function of time and temperature. It takes care of involving the ionic strength effect and Arrhenius expression in the rate constants correction. The results show a fast decay of $HO^{\bullet}$ yields in the 10^{-10}-10^{-8} s range which denotes an efficient reactivity of this species in the track structure of the ion beam. This effect is enhanced with the lowest LET of O^{8+}. Increasing temperature also accelerates the decays for both ions. These observations are discussed in terms of temperature activation of reactions and the track structure exhibiting the formation of $HO^{\bullet}$ in a "low LET" penumbra around the ionization tracks. $HO^{\bullet}$ track segment yields at 100 ns, of 0.4×10^{-7} and 0.6×10^{-7} mol/J, respectively for 350 and 65 eV/nm, are not affected by temperature.

TOC GRAPHICS

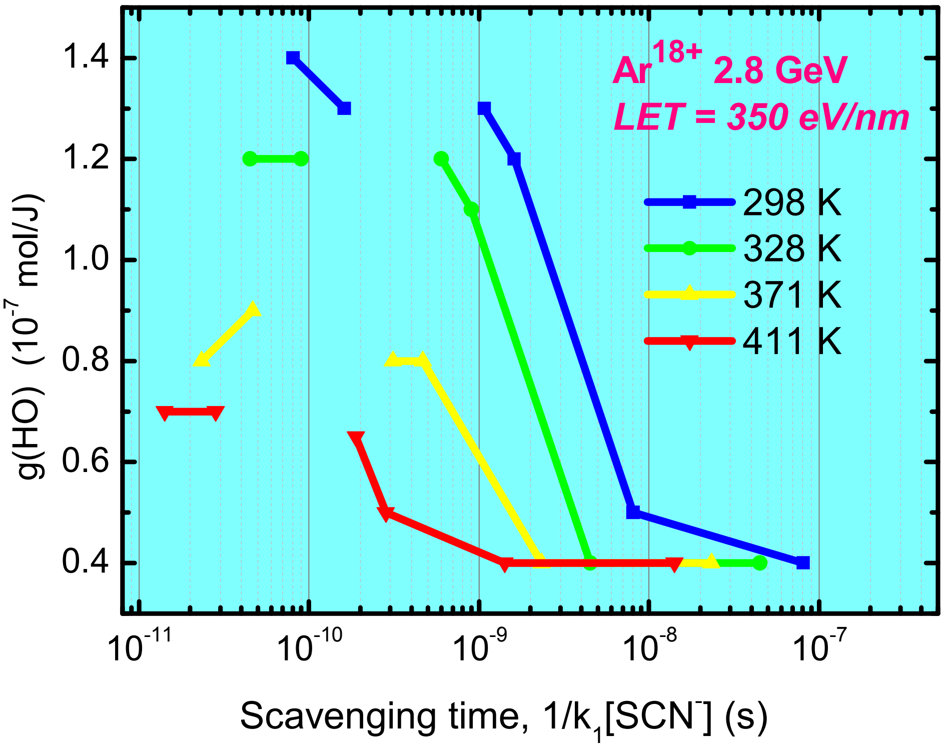

KEYWORDS: Hydroxyl radical, LET effect, Temperature, Scavenging method, Pulse radiolysis, Potassium thiocyanate.

Introduction

Hydroxyl radical ($HO^\bullet$) is a very powerful oxidant having a standard potential of 1.9 V in neutral aqueous solution.[1] It is formed in water under energetic radiation.[2] Its lifetime is also very short due to its reactivity against almost any material. It can be particularly unwelcome when it leads to biological materials damages (DNA damage for instance)[3] or to corrosion/degradation of confinement envelops (corrosion of alloys used in nuclear reactors for instance). $HO^\bullet$ is also viewed in a positive way when it is used to kill tumors in radiological treatment of cancers. Medical research even tries to multiply this species (its effects) nearby the tumor by using nanoparticles.[4,5] From the $HO^\bullet$ reactivity point of view, it can also recombine with itself to form hydrogen peroxide (H_2O_2) and more generally it is involved in the complex chemical mechanism of water radiolysis : a reaction system involving at least 30 significant reactions in pure water.[6] Knowing the radiolytic yields (G) of radical species in radiation chemistry is essential to predict the fate of secondary chemical species at short (ns) and long terms (years).[6] Among the parameters that influences the G-value, the temperature T and the Linear Energy Transfer ($\mathrm{LET} = -\frac{dE}{dx}$) that defines the way how the energy E is deposited by the incident particle in water along its propagation axis (x), are very strategic in nuclear industry. Their effects are often coupled.

Despite of a few examples of experimental and theoretical researches, the chemistry of $HO^\bullet$ at elevated temperature is still not established in water radiation chemistry under high Linear Energy Transfer (LET) radiations (energetic α-rays, neutrons, recoil ions).[7,8] However, $HO^\bullet$ is the only species to consume the radiolytic H_2.[9] Actually, water radiolysis in nuclear water reactors crucially misses the $HO^\bullet$ radiolytic yield in the extreme conditions which characterize nuclear power reactor: high temperatures (typically from boiling conditions to 583 K, 11 MPa) up to supercritical conditions, combined radiations of low and high LET, high dose rates, etc....[9] Nevertheless the crucial parameters Temperature and LET were independently examined. A collection of rate constants and radiolytic yields from Elliot and Bartels' report became the reference in terms of the effect of temperature on radiation chemistry of water.[8] More recent data expand the range of temperature in investigations going to the supercritical domain, over 374°C, 22 MPa.[10] It is well established that the yield of $HO^\bullet$ increased with rising temperature under low LET radiations (γ-rays, high energy electrons).[8,11] Primary radiolytic yields of $HO^\bullet$ (escaped from spurs recombinations) were evaluated from 2.7×10^{-7} mol/J at ambient temperature to 5×10^{-7} mol/J at 350°C.[11] From the simulation point of view, at least two different approaches exist: Monte Carlo simulations and diffusion-kinetics modelling.[12-20] Both simulations have suggested a reaction model explaining the observed excess of H_2 produced above 200°C under low LET radiations.[17,20] This reaction model implies also an excess production of $HO^\bullet$ which was never observed experimentally but more and more admitted after a controversial period on the rate constant estimation of a delayed $HO^\bullet$ formation by the reaction $H^\bullet+H_2O \rightarrow HO^\bullet+H_2$.[20-23]

The influence of LET on radiation chemistry of water has been extensively studied during these last 30 years by using several kinds of energetic heavy ions (various charges, masses and energies), in two different ways: steady state and pulse radiolysis.[24-26] It was taught that radiolytic yields of radical species decrease with increasing LET and inversely for molecular species (H_2 and H_2O_2). It is due to the initial structure of energy deposition which depends on the charge and the velocity of ions, that involves dense domains of ionizations where the recombinations of radicals are favored.[27] $HO^\bullet$ radicals were never observed directly in the tracks unlike hydrated electrons by pulse radiolysis.[28-32]

We conclude that temperature effects were investigated mainly with low LET radiations and pulse radiolysis since the 80s[33] and that only recent experiments in reactor start to bring new approaches under combined radiations.[34,35] However temperature and LET have inversed effects on the radiolytic yields of $HO^{\bullet}$. It is therefore expected a competition when LET and T increases, between the acceleration of recombinations in the track and the escape of species with the increase of diffusion. This should depend strongly on the track structure. That fast non homogeneous chemistry must be also investigated by using a time resolved method for accessing to the ps-ns time scales.

It is then presented in this article the first experimental results on the temperature dependence of $HO^{\bullet}$ radical yield along its formation/consumption history, in water irradiated with high LET radiation. It is carried out over the range 298-411 K and by using energetic ions $^{36}Ar^{18+}$ of 3.4 GeV and $^{16}O^{8+}$ of 1.2 GeV in order to interpret the results in terms of the track expansion of a segment of energy deposition having various LET values different from MeV γ-rays (0.3 eV/nm).[24,36] These kinds of radiation are not penetrating enough in existing high temperature optical cell.[37-39] Development of new high temperature cell for heavy ion is then necessitated.

Because of the low extinction coefficient of $HO^{\bullet}$ in UV[40] and the expected low yields at high LET[30], we have not chosen the direct detection of $HO^{\bullet}$. Nevertheless in order to determine the radiolytic yield of $HO^{\bullet}$ versus time, the scavenging method with thiocyanate (SCN^-) is convenient.[30,41] Radiolysis of SCN^- is sufficiently known[42-44] and already studied in the radiolysis at high temperature[45,46] to trust in its mechanism and rate constants within the limits of temperatures of previous investigations.[45] Other organic chemical systems would have been chosen for their sensitivity by using fluorescence or optical transmission detection but they are not stable enough at high temperatures and fluorescence could become less sensitive at high temperature.[32,47-53] Formic acid solutions would have been another possibility of scavenging but analysis of CO_2 in the gas phase would also be more difficult with a temperature effect implementation.[54,55] More-over the first data concerning the using of SCN^- under energetic radiation different than electron beam come from the experiments of Chitose *et al.*[56], when proton pulses of 5.2 MeV energy were used. Baldacchino *et al.*[30] investigated as well SCN^- solutions under the action of high energy C^{6+} and Ar^{18+}. Such high interest in SCN^- is due to the fact that it can be easily oxidized to $(SCN)_2^{\bullet-}$ through the following reactions:

$$HO^{\bullet} + SCN^{-} \rightarrow HOSCN^{\bullet-} \qquad \text{Reaction 1}$$

$$HOSCN^{\bullet-} \rightleftharpoons SCN^{\bullet} + OH^{-} \qquad \text{Reaction 2}$$

$$SCN^{-} + SCN^{\bullet} \rightleftharpoons (SCN)_2^{\bullet-} \qquad \text{Reaction 3}$$

$$2(SCN)_2^{\bullet-} \rightarrow (SCN)_2 + 2SCN^{-} \qquad \text{Reaction 4}$$

$(SCN)_2^{\bullet-}$ is formed during the radiation pulse and disappears with a slow dismutation reaction (reaction 4) that makes this species observable in the microsecond time range. This time range is delayed from the occurrence of reaction (1) which is the reaction of interest for the evaluation of $HO^{\bullet}$ yield. More-over its absorption coefficient is high enough for time resolved absorption spectroscopy: 7600 $M^{-1}cm^{-1}$ at 475 nm at ambient temperature. Temperature dependence of $(SCN)_2^{\bullet-}$ spectrum was examined.[45,46] and it was shown a 30% decrease of molar absorption coefficient between 298 K and 673 K at 475 nm.

The scavenging method used in our study, consists in varying the concentration of SCN^- and in determining the $HO^{\bullet}$ radiolytic yield for each concentration (i.e the scavenging time). Deconvolution is made by taking into account the rate constant of the above mentioned reactions and by adjusting $g(HO^{\bullet})$ (time dependent radiolytic yield of $HO^{\bullet}$) for simulating the formation and the decay of $(\mathrm{SCN})_2^{\bullet-}$. We will see that is mandatory to recalculate the rate constants and the absorbance by considering the effect of temperature and the ionic strength.

Experimental method

In the present work six concentrations of KSCN were investigated: 1 mM, 10 mM, 50 mM, 75 mM, 0.5 M and 1 M. The chemical reagents were purchased from Sigma-Aldrich and used without further purification. The purity of KSCN was greater than 99.9%. Ultra-pure water (18.2 MΩ·cm) from Milli-Q Millipore System was used to prepare the solutions directly before experiment without pH buffer. All solutions were air saturated.

Pulse radiolysis experiments were performed at the Grand Accélérateur National d'Ions Lourds (GANIL, Caen – France) cyclotron.[31] Swift ions of $^{36}\mathrm{Ar}^{18+}$ and $^{16}\mathrm{O}^{8+}$ were used as a pulsed irradiation source in two separate experiments but by using the same setup. The pulse duration of ion beams was 10 μs and the repetition rate was 100 Hz. The initial energies of $^{36}\mathrm{Ar}^{18+}$ and $^{16}\mathrm{O}^{8+}$ were 95 MeV/nucleon (3.4 GeV) and 75 MeV/nucleon (1.2 GeV) respectively.

Knowing that the penetration of energetic heavy ions is much smaller than the penetration of γ-rays or accelerated electrons, it is required to design an optical cell that has relatively thin input window that allows penetrating ionizing radiation through the solution. Figure 1 presents some details of this optical flow cell. For this study an optical cell was designed by HP System company to afford high temperature (up to 450°C), high pressure (up to 50 MPa) and irradiation by high-energy heavy ions. It constitutes an "open" autoclave that allows circulating an aqueous solution. It was made of Inconel 718 alloy, known as highly resistant to corrosion and having a low dilatation coefficient at elevated temperatures. Its main body has a cylindrical shape of 51 mm length with external and internal diameter of 51 and 1.5 mm, respectively. The irradiation port is made of a window of 3 mm of effective diameter and 0.345 mm of thickness machined in

Inconel to let energetic ions to pass. To hold high pressure, the shape of this window is spherical with a curvature turned inside the cell (details are shown in Figure 1b). On the edges of this window energetic ions may stop in a thicker material which reduces the effective irradiation beam diameter to 2 mm.

Simulations of energy depositions, in term of LET along the ion beam trajectory inside the solution/irradiation interaction chamber, performed with SRIM program[57] are presented in Figure 2. The initial energies of ions after crossing the irradiation port windows (Inconel of 0.345 mm of thickness) are 2.8 GeV and 1.08 GeV respectively. LET does not change a lot along the 1.5 mm in the solution. An average value of LET in the track segment of 1.5 mm can be estimated for $^{36}Ar^{18+}$ and $^{16}O^{8+}$ as 350 eV/nm and 65 eV/nm respectively. The ion charge is considered as constant in this track segment, in SRIM calculations. The initial beam diameter was 3 mm. According to the physical dosimetry performed during irradiation by a secondary electron detector that was initially calibrated with the current of a Faraday Cup placed into the beam, the dose was estimated to be 100 Gy per pulse. Variations of ±10 Gy were noticed from one experiment to another during the current monitoring. As specified below, beam diameter is reduced in diameter by the window curvature to 2 mm. That reduction implies a dose reduction to an estimated value of 70-80 Gy. This value will be adjusted for the ambiant temperature result for which we have already an estimation of $HO^{\bullet}$ yield (*vide infra*).

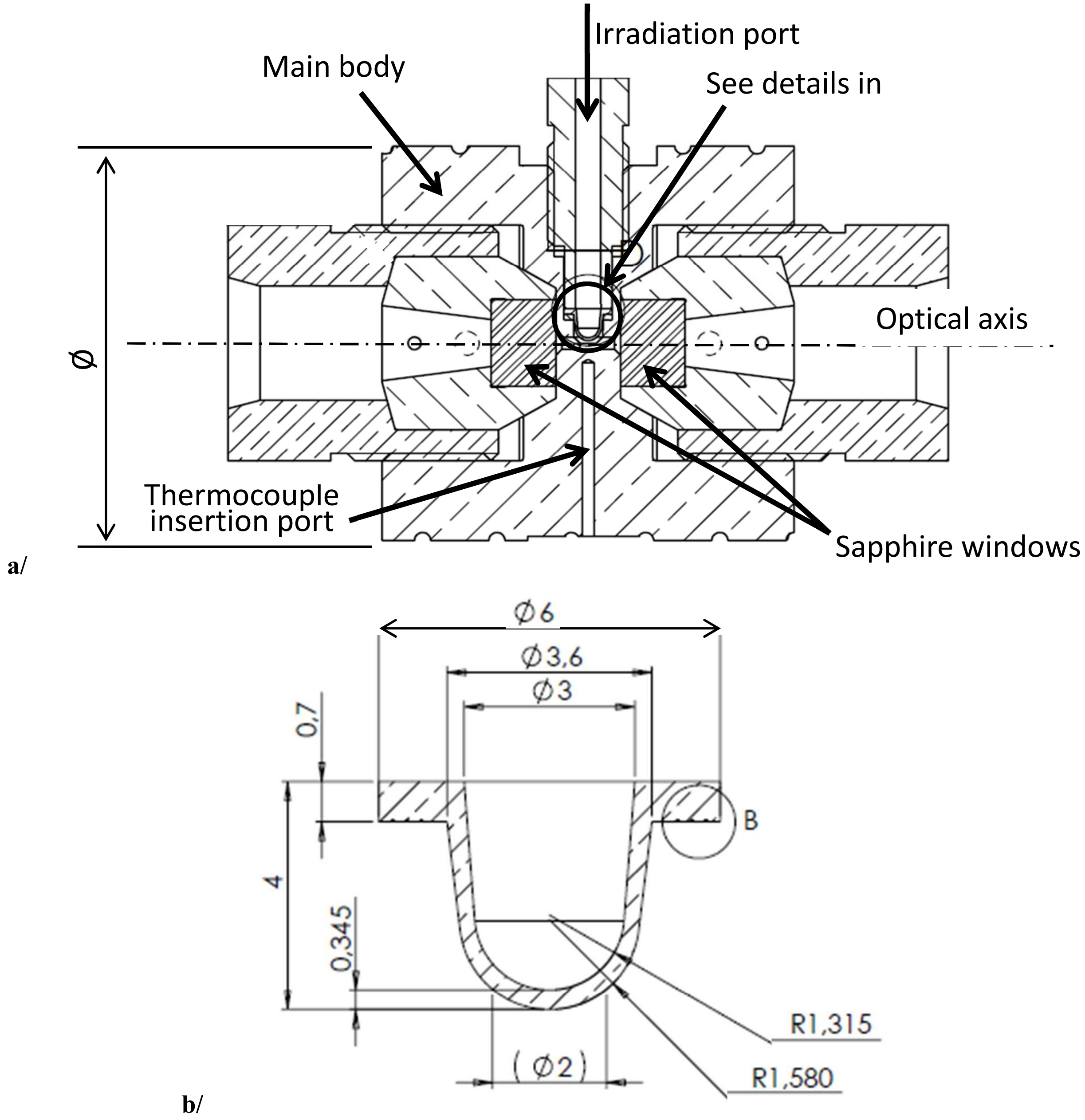

Figure 1. Scheme of the whole irradiation optical flow-cell resistant to temperature (450°C max) and pressure (50 Mpa max), viewed from the top (a). Dimensions are mentioned in the text. Details of the irradiation port are given in inset (b); dimensions are given in mm.

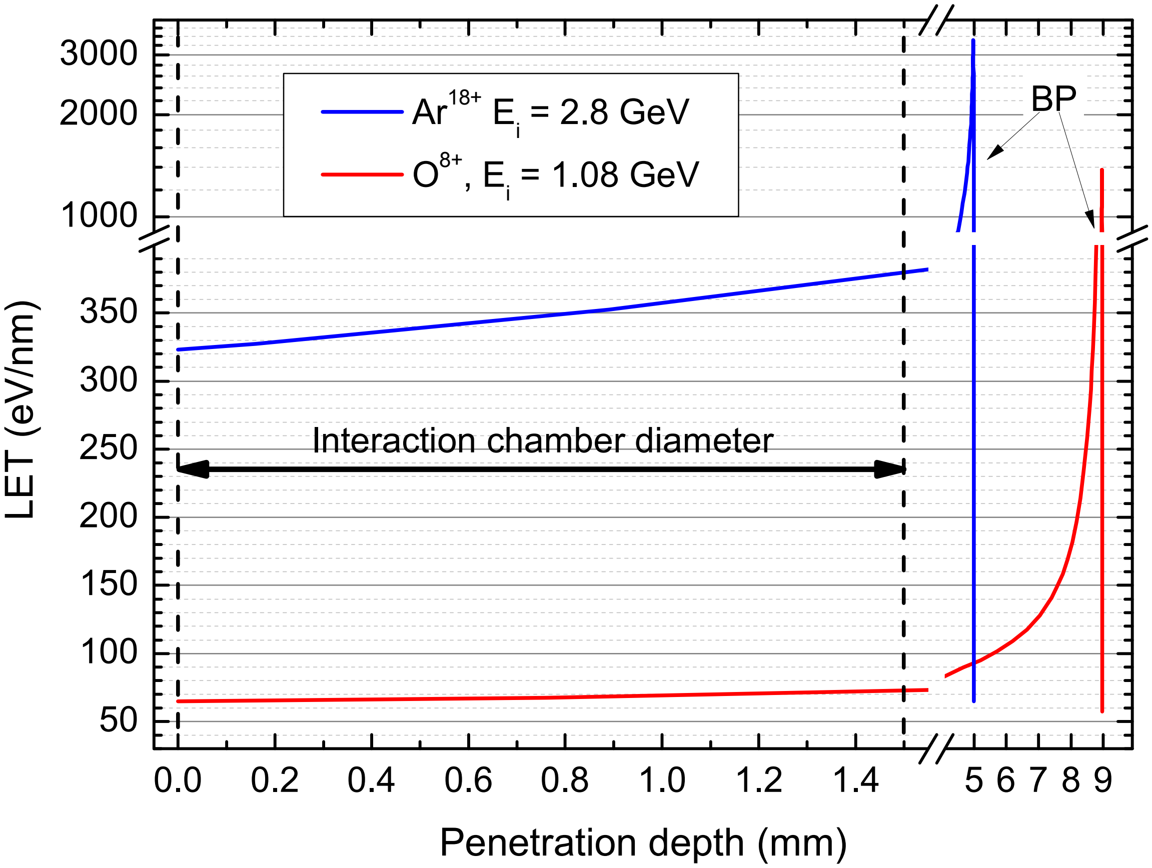

Figure 2. Energy deposition of Ar^{18+} and O^{8+} ions of incident energies (E_i) of 2.8 and 1.08 GeV respectively, in water, calculated with SRIM program. The interaction chamber segment (1.5 mm) is zoomed to analyze the slight evolution of LET far from the Bragg peak (BP) which exhibits very high LET values.

Along with the optical path two sapphire windows that transmit the analyzing UV-visible light are placed. Sapphires are placed in a support head made of Inconel which is pressed against the cell body with a screw (a typical couple of 70 Nm is used) for sealing. They were never changed during the experiments. A solution flow of 1 cm^3/min is provided by an HPLC pump (PU-2080-100, Jasco) associated to a backpressure regulation (BP-2080, Jasco). All experiments were performed at constant pressures of 25 MPa and 15 MPa for Ar^{18+} and O^{8+} experiments respectively[1]. This pumping system was already described in the literature.[39,58] A residence time in front of irradiation beam of solution can be estimated to 0.21 s which long enough for investigating two orders of magnitude less kinetics. The cell heating was applied by two formable coil heaters having a power of 215 W and including a J-thermocouple for regulation (Ivaldi). The temperature was measured close to the interaction chamber with a K-thermocouple. Two independent temperature regulators (Watlow Series 980) allowed a stability of 1°C inside the cell with a sample flow of $1 cm^3$/min. A remote control of temperature and pressure was made by using a homemade PC-program.

Real time absorption spectroscopy was performed along the 2 mm optical pathway that is defined by the irradiation beam diameter (*vide supra*). Two kinds of analyzing light were used for the data set acquisitions for Ar^{18+} and for O^{8+}. A CW Xe-arc lamp (Oriel 150W) was used as analyzing light for Ar^{18+} experiments. It was coupled to a 20m-length optical fiber and was lead to the optical cell and focused into it. The transmitted light was lead to a monochromator (HR25, Jobin Yvon) through another 20 m-length optical fiber. The absorbance of $(SCN)_2^{-\bullet}$ was measured at 475 nm. The detection was performed by a photomultiplier (R928S, Hamamatsu). For O^{8+} experiments, a 200 mW CW DPSS 532nm laser (OXXIUS Laserbox) was used instead of the lamp. Therefore monochromator and photomultiplier were both replaced by a pin diode couple to the fiber. This change has improved the signal to noise ratio and due to the wavelength, absorption coefficients will be adapted. In both cases the intensity variation was recorded by using a 40 GS/s oscilloscope (DPO-7254, Tektronix) with an input impedance of 10 kΩ. Record

---

[1] In the temperature range of 298-425K, density of water has been calculated on the base of IAPWS-IF97 formulation: at 298 K, 1.003 (15 MPa) and 1.007 (25 MPa); at 425 K, 0.925 (15 MPa) and 0.930 (25 MPa). The variations between 15 and 25 MPa, lower than 0.5%, were not considered in the analysis part.

lengths include over a million of data that were averaged to obtain kinetics with only 500 points. This operation was performed in addition of a thousand of accumulations to increase significantly the signal to noise ratio. The triggering signal was provided by the cyclotron electronics.

Results

The results are focused on the time dependence of $HO^{\bullet}$ track segment yield at various temperatures. The kinetics are carried out by using pulse radiolysis technique with a pulsed beam of ions. The pulse trains of 10 μs were delivered by GANIL cyclotron at Caen/France. This method was combined with the scavenging method.

As it is reported in Figure 3 for Ar^{18+} ions, transient absorption at 475 nm of $(SCN)_2^{\bullet-}$ is recorded over the microsecond range and for an initial concentration of SCN^- of 0.001 M, for four temperature values 298, 328, 371 and 411 K. $(SCN)_2^{\bullet-}$ formation is completed in the irradiation pulse (10 μs) and the decay follows the second-order reaction 4. When temperature increases, the absorbance of $(SCN)_2^{\bullet-}$ corresponding to scavenged $HO^{\bullet}$ radical decreases. It is first due to the molar absorption coefficient of $(SCN)_2^{\bullet-}$ that decreases with the increase of temperature at 475 nm.[45,46] Due to the second order of reaction 4 (dismutation of $(SCN)_2^{\bullet-}$) the observed rate constant strongly depends on the initial concentration of $(SCN)_2^{\bullet-}$ which is formed in the pulse. This concentration directly depends on $HO^{\bullet}$-yield as well. Such decrease of the absorbance may be then caused by the acceleration of the recombination reaction of $HO^{\bullet}$ at elevated temperature, and by the initial track structure which is supposed to be dense at earliest time for high LET particles. On the other hand, a faster decay of $(SCN)_2^{\bullet-}$ with increasing temperature is not clear without any detailed analysis. It was normally observed in previous low LET investigations.[46]

These current results would reveal the initial concentration of $HO^{\bullet}$ is about 10^{-6} M which is much lower than the concentration of $HO^{\bullet}$ obtained by Wu *et al.*[46] That is nevertheless an expected behavior because of the high LET value of $^{36}Ar^{18+}$ particles.

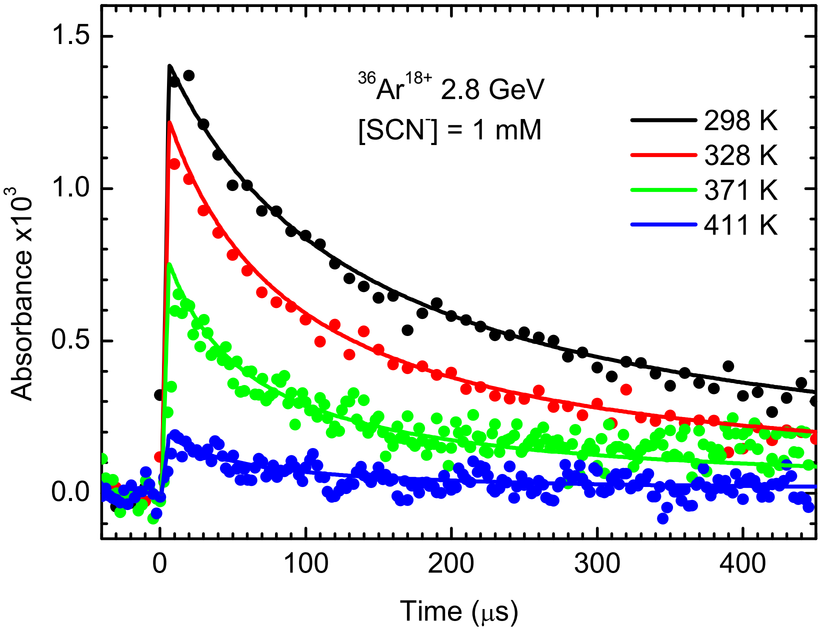

Figure 3. Absorbance kinetics of $(SCN)_2^{\bullet-}$ in 1 mM K^+SCN^- solution at 298, 328, 371 and 411 K. Dose wass 80 Gy in the 10 µs of $^{36}Ar^{18+}$ pulse. Wavelength was 475 nm and path-length 2 mm. Flow was 1 cm^3/min. Line plots are performed by Chemsimul® program following the protocol described in the Data analysis section.

Unlike Ar^{18+} ions, kinetics of $(SCN)_2^{\bullet-}$ dismutation obtained for O^{8+} ions (Cf. Figure 4) seem clearly to be accelerated by temperature. The values of absorbance are lower than for Ar^{18+} ions (below 10^{-3}) but it can be roughly explained by a lower dose per pulse (20 Gy instead of 80 Gy for Ar^{18+} ions) which is slightly compensated by an expected higher value of $HO^{\bullet}$ yield for a lower LET value (65 instead of 350 eV/nm). At 532 nm, absorption coefficient of $(SCN)_2^{\bullet-}$ also increases with temperature because of the red shift of the spectrum when temperature increases.[45,46]

In order to set the scavenging method[59], kinetics were recorded by using various concentrations of the HO$^\bullet$-scavenger, SCN$^-$. In Figure 5, kinetics are presented under pulsed irradiation by O^{8+} and temperature of 365 K. Concentration range was 1 mM to 1 M which covers a range of scavenging time going roughly from 50 ps to 50 ns.

The influence of initial concentrations of SCN$^-$ concerns both amplitude of the absorbance and decay. For a given temperature, absorption coefficient does not change. Then the maximum of absorption is deduced from HO$^\bullet$ yield and the chemical kinetics during the dose delivery in the pulse. There is not a natural behavior of this maximum unlike the decay which seems to be accelerated by the concentration increase. A rational analysis of this kinetics set must be done to show the evolution of HO$^\bullet$-yield versus time.

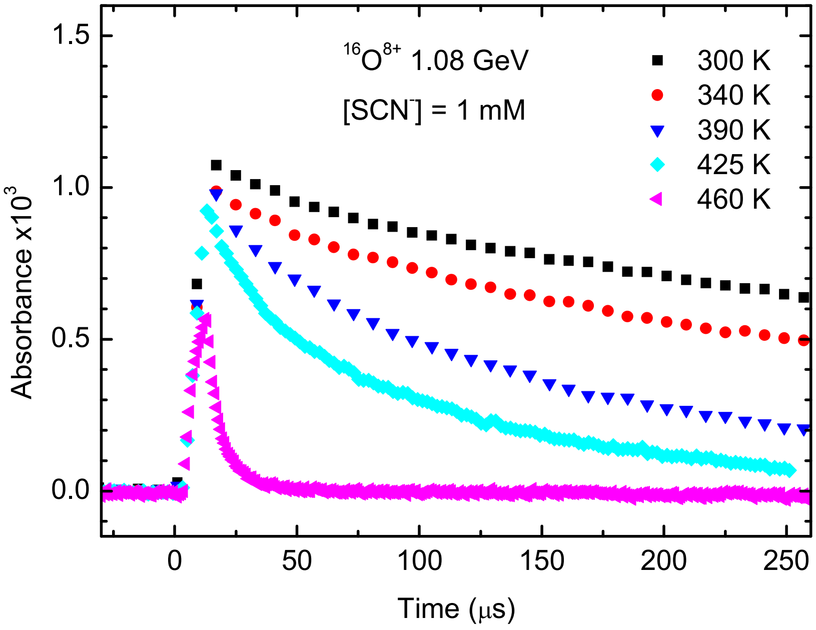

Figure 4. Absorbance kinetics of $(SCN)_2^{\bullet-}$ in 1 mM K$^+$SCN$^-$ solution at 300, 340, 390, 425 and 460 K. Dose is 20 Gy in the 10 µs of $^{16}O^{8+}$ pulse. Wavelength was 532 nm and path-length 2 mm. Flow was 1 cm^3/min.

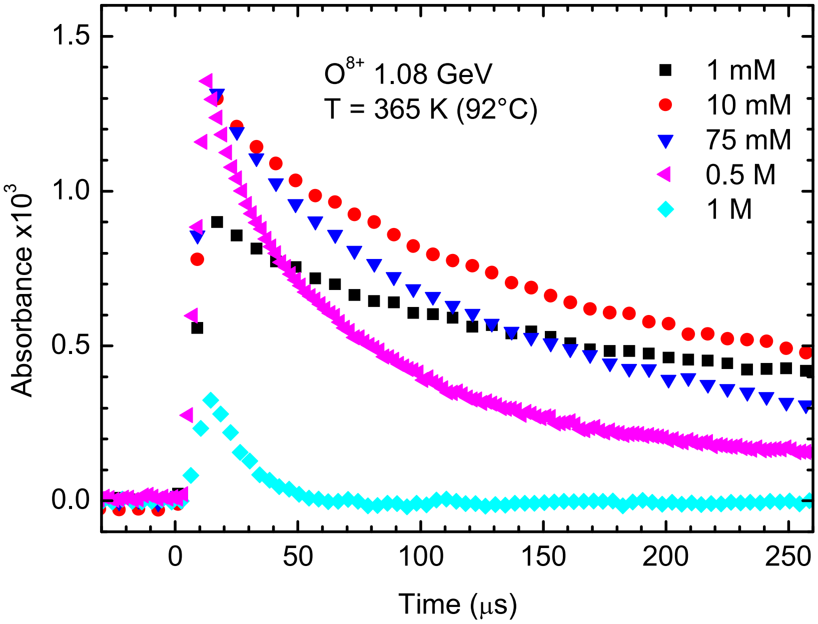

Figure 5. Absorbance kinetics of $(SCN)_2^{\bullet-}$ at 365 K (92°C) for five concentrations of K^+SCN^- : from 1 mM to 1 M. Dose is 20 Gy in the 10 μs of $^{16}O^{8+}$ pulse. Wavelength was 532 nm and path-length 2 mm. Flow was 1 cm^3/min.

Data analysis

The purpose of this analysis is to determine the radiolytic yield of hydroxyl radical for different temperature and different scavenging power of SCN^-. g($HO^\bullet$) has been determined by using deterministic simulation for fitting kinetics. In order to analyze the formation and decay of $(SCN)_2^{-\bullet}$ we have used Chemsimul®,[60] a computer program for simulation of chemical reactions.

Authors made the hypothesis that the whole reaction system of water under radiation does not necessitate to be implemented in the calculation except the water dissociation equilibrium as it was depicted in the article of Wu *et al.*[46] Actually we also supposed that reactions 1 to 4 do not interfere with radicals/molecules in the track reactions unlike it was suspected when this system was used at elevated scavenging capacities under high LET irradiation.[56]

In order to adjust the experimental data to simulation kinetics, we fixed the parameters such as the measured irradiation dose and the fixed optical path. We adjusted the value of molar absorption coefficient of $(SCN)_2^{-\bullet}$ to the temperature by using the evaluations of Wu *et al.*[46] The radiolytic yield, $G(HO^\bullet) = 0.4\times10^{-7}$ mol/J deduced from the data obtained by Baldacchino *et al.*[29,30] for hydrated electron yields and for $HO^\bullet$-yields in 1 mM of SCN^- condition, with similar Ar^{18+} irradiations, was taken as reference value at ambient temperature because there were close conditions of ion beam.

Temperature and ionic strength must be taken into account for correction of the rate constants in the model used in the yield de-convolution. Reactions 1 to 4 presented in introduction play important roles in the mechanism when temperature and concentration increase. It is then of great importance to describe as well as possible the equations that provide the rate constants for each chemical equation. Table 1 collects the critical parameters for Arrhenius equation and equilibrium constants calculation. E_a is the Activation Energy, A is the pre-exponential factor and K_i is equilibrium constant, used for Reaction i ($i = 2$ or 3). Arrhenius law is the most representative and commonly used in the range of temperature currently investigated (298-450 K). Other expressions of rate constant function of temperature exist for wider ranges of temperature.[61] Nevertheless the parameters corresponding to these expressions are not available in literature for the current mechanism.

Rate constant of reaction 1 (k_1) was calculated taking into account Arrhenius parameters defined in Table 1. They are presented in Table 2 for four different temperatures. Rate constants for equilibria 2 and 3, also presented in Table 2 for the same temperatures, were calculated by taking into account thermodynamic parameters ($\Delta H°$, $\Delta S°$).

TABLE 1. Parameters and reference used for calculation of k_1 to k_3. Arrhenius equation (Ln $k = \mathrm{Ln}\ A - E_a/\mathrm{RT}$) and thermodynamic parameters (Equilibrium constant K and Gibbs enthalpy calculation) are collected. R is the gas constant (8.3144722 $\mathrm{J \cdot K^{-1} \cdot mol^{-1}}$) and T the temperature in Kelvin.

$HO^{\bullet} + SCN^{-} \rightarrow HOSCN^{\bullet -}$	k_1	Ln A = 29.614, E_a/R = 1900 K	Chin *et al.*[42]
$HOSCN^{\bullet -} \rightarrow SCN^{\bullet} + OH^{-}$	k_2	$k_2 = 2.0\times10^{8}\ \mathrm{s^{-1}}$	Wu *et al.*[46]
$HOSCN^{\bullet -} \leftarrow SCN^{\bullet} + OH^{-}$	k_{-2}	$k_{-2} = k_2 / K_2$, with Ln $K_2 = (16000+77\times T) / (\mathrm{R}\times T)$	
$SCN^{-} + SCN^{\bullet} \rightarrow (SCN)_2^{\bullet -}$	k_3	Ln A = 23.459, E_a/R = 271 K	Chin *et al.*[42]
$SCN^{-} + SCN^{\bullet} \leftarrow (SCN)_2^{\bullet -}$	k_{-3}	$k_{-3} = k_3/K_3$, with Ln $K_3 = (36800+21.94\times T) / (\mathrm{R}\times T)$	[46,62-64]
$2(SCN)_2^{\bullet -} \rightarrow (SCN)_2 + 2SCN^{-}$	k_4	Ln A = 26.15, E_a/R = 1564 K	Elliot *et al.*[45]

For calculating the rate constant of reaction 4 (dismutation of $(SCN)_2^{\bullet -}$), the ionic strength and the change of dielectric constant for varying temperature must also be considered. Actually this is a reaction between ions which is sensitive to ionic strength.[65]

TABLE 2. Calculated values of k_1 to k_3 by using Arrhenius equation and thermodynamic parameters given in Table 1, by changing the temperature. Unit is $\mathrm{M^{-1}s^{-1}}$ except for k_2 in $\mathrm{s^{-1}}$.

T	**298 K**	**328 K**	**371 K**	**411 K**
k_1	1.24×10^{10}	2.2×10^{10}	4.35×10^{10}	7.15×10^{10}
k_2	2×10^{8}	2×10^{8}	2×10^{8}	2×10^{8}
k_{-2}	3.31×10^{9}	5.97×10^{9}	1.18×10^{10}	1.95×10^{10}
k_3	6.21×10^{9}	6.75×10^{9}	7.43×10^{9}	7.98×10^{9}
k_{-3}	3.11×10^{4}	1.31×10^{5}	6.89×10^{5}	2.36×10^{6}

In the Debye-Hückel theory which is described in several Chemical Kinetics books[66,67], the ionic strength I is defined, following G.N. Lewis, by the equation: $I = \frac{1}{2}\sum C_i Z_i^2$, where C_i is the concentration of the ionic species i and Z_i its charge. In our case, $I = [SCN^-]$. Only k_4 is concerned by a correction with the ionic strength. At room temperature, an extended development can express a corrected constant, k'_4, as a function of ionic strength and the charge of reactants (2 x $(SCN)_2^{-\bullet}$): $Z_a = Z_b = -1$, then

$$\ln k'_4 = \ln k_4 + 1.02\, Z_a Z_b \sqrt{I}\,/\left[1 + \sqrt{I}\right] \qquad \text{Equation 1}$$

In the book of Weston and Schwarz[65], a development of the formula is proposed through the expression of the ionic radius $\kappa^{-1}$of the ionic reactant atmosphere. κ^{-1} is a function of temperature T and the dielectric constant (or relative permittivity) ε, itself depending on T. The expression has been clearly written in articles[46,68,69] to give:

$$\ln k'_4 = \ln k_4 + 8.38 \times 10^6\, Z_a Z_b f(I)\,/(\varepsilon T)^{3/2} \qquad \text{Equation 2}$$

with $f(I) = \sqrt{I}/\left[1 + B\sqrt{I}\right]$,

and $B^2 = (\varepsilon T)_{293}/(\varepsilon T)_T$

ε have been tabulated from Handbook data at various temperatures and have been included in the calculation of k'_4. Corrected k'_4 are reported in Table 3. They were calculated according to Equation 1 presented below[68-70], ε is the relative dielectric constant at temperature T (K). The applicability of Equation 2 is connected to $\sqrt{I}$ which must be less than approximately 0.3 (depending on the species). In the case of 0.5 and 1 M of SCN^-, the Debye-Hückel theory foresees a reduction of the I value because, for instance, of the formation of pairs. The consequences are typically the rate constants decrease instead of increase with *I*. Observing the kinetics in Figure 5, for 0.5 and 1 M, we cannot see this type of behavior because of faster and faster decrease of $(SCN)_2^{-\bullet}$.

TABLE 3. Calculated values of k'_4 by using Equation 2 by varying the concentration (ionic strength) and the temperature. Unit is $M^{-1}s^{-1}$.

SCN^- Conc.	**0.001 M**	**0.01 M**	**0.05 M**	**0.075 M**	**0.5 M**	**1 M**
298 K	1.29×10^9	1.48×10^9	1.84×10^9	1.98×10^9	3.16×10^9	3.86×10^9
328 K	2.03×10^9	2.36×10^9	2.96×10^9	3.20×10^9	5.22×10^9	6.43×10^9
371 K	3.67×10^9	4.34×10^9	5.59×10^9	6.10×10^9	1.04×10^{10}	1.31×10^{10}
411 K	5.58×10^9	6.73×10^9	8.92×10^9	9.83×10^9	1.77×10^{10}	2.26×10^{10}

Fittings were performed by using Chemsimul® than calculates the kinetics by integrating the chemical mechanism (reaction 1 to 4) with the reaction rates, and the parameters corresponding to the formation of $HO^\bullet$ radicals: dose, duration of the pulse and $HO^\bullet$-yield. As a basic result Chemsimul gives a plot of time versus concentration of $(\mathrm{SCN})_2^{\bullet-}$. This plot can be transformed in optical density by multiplying the concentration by the product “absorption coefficient” × “optical path length”. Adjustment to experimental kinetics is performed by changing $HO^\bullet$-yield. Dose may also be changed when beam intensity changed. Examples of adjustment are given in Figure 1.

Discussion

Figure 6 reports $HO^{\bullet}$-yields under Ar^{18+} ions irradiation of 350 eV/nm, as a function of the scavenging time by SCN^-. The SCN^- concentration range is 1 mM to 1 M which corresponds to a scavenging range of 7×10^{-7} to 7×10^{-11} s at room temperature. This scale is shifted when increasing the temperature because the value of k_1 is greater. At 298 K, for the longest time, the yield value has been fixed by considering the values of $g((SCN)_2^{\bullet-})$ in N_2O saturated solutions[30] and the values of $g(e^-_{aq})$ published with the same ion beam[29]. In N_2O saturated solutions the yield is the sum $g(HO^{\bullet})+g(e^-_{aq})$ thus we can deduce $g(HO^{\bullet})$. LET values in these articles (280 eV/nm) are slightly different than 350 eV/nm. That should decrease again the $HO^{\bullet}$-yields of about a few percent in this current study which remains in our present relative accuracy. Then at 100 ns, $g(HO^{\bullet})$ should have a value of 0.4×10^{-7} mol/J. For the kinetics at 298 K, the dose value has been adjusted and confirmed at 80 Gy per pulse which was independently determined by the ion counting. Nevertheless, the yields at earliest times reach $1.2\text{-}1.3\times10^{-7}$ mol/J in the nanosecond scale, whereas Baldacchino *et al*. found these same values at 10^{-10} s.[30] At these high scavenging capacities, de-convoluting the chemical kinetics becomes important[43] and the effect of ionic strength must be corrected. Unfortunately Baldacchino *et al.* did not perform this de-convolution in 2006.[30] That is probably why the yields were under estimated.

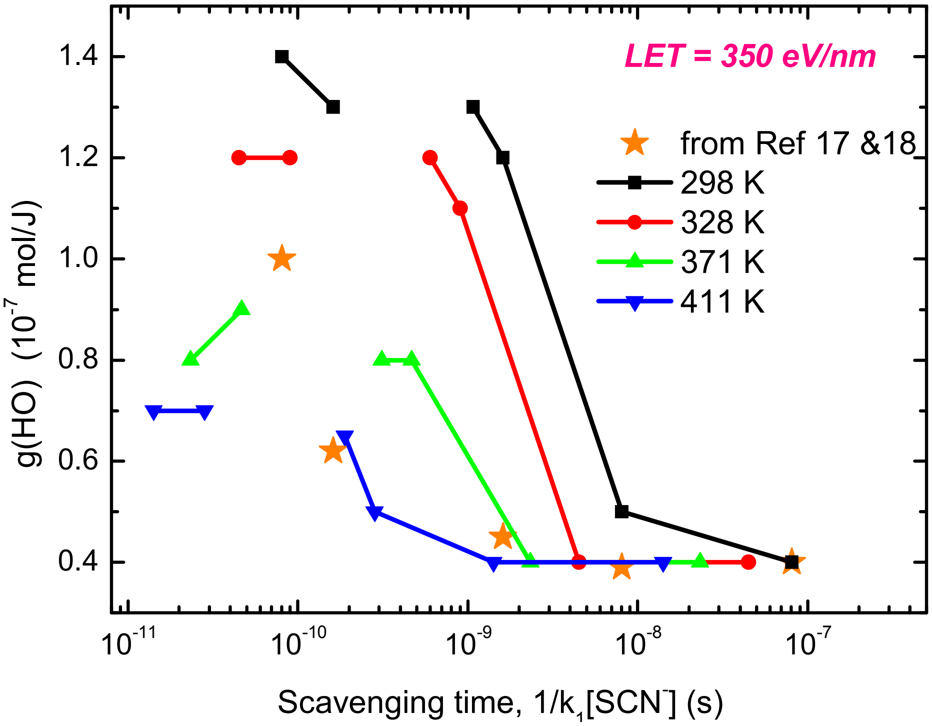

Figure 6. Radiolytic yield of $HO^\bullet$ as a function of scavenging time at 298, 328, 371 and 411 K for irradiation with Ar^{18+} ions having 350 eV/nm of LET. Shortest times corresponding to the scavenger concentrations of 0.5 and 1 M are disconnected from the other data because of the non-applicability of the Debye-Hückel ionic strength correction. Data from references 17 and 18 are given at ambient temperature.

Figure 7 reports $HO^\bullet$-yields under O^{8+} ions irradiation of 65 eV/nm, as a function of the scavenging time by SCN^-. At low scavenging capacity, i.e. at 100 ns, the $HO^\bullet$-yield is 0.6×10^{-7} mol/J. This yield is greater than that at 350 eV/nm and lower than that at 32 eV/nm (an estimation of $1.1\text{-}1.2\times10^{-7}$ mol/J on the basis of a recent publication[30]). It is also lower than the yields determined with higher energy ions[50] (about 1.1×10^{-7} mol/J). Moreover it is independent on temperature in the investigated range of 298-368 K. A small increase at 408K is observed but authors do not want to trust too much this value because of the bad signal to noise ratio in this experiment. The relative accuracy of this adjustment was estimated to 50%.

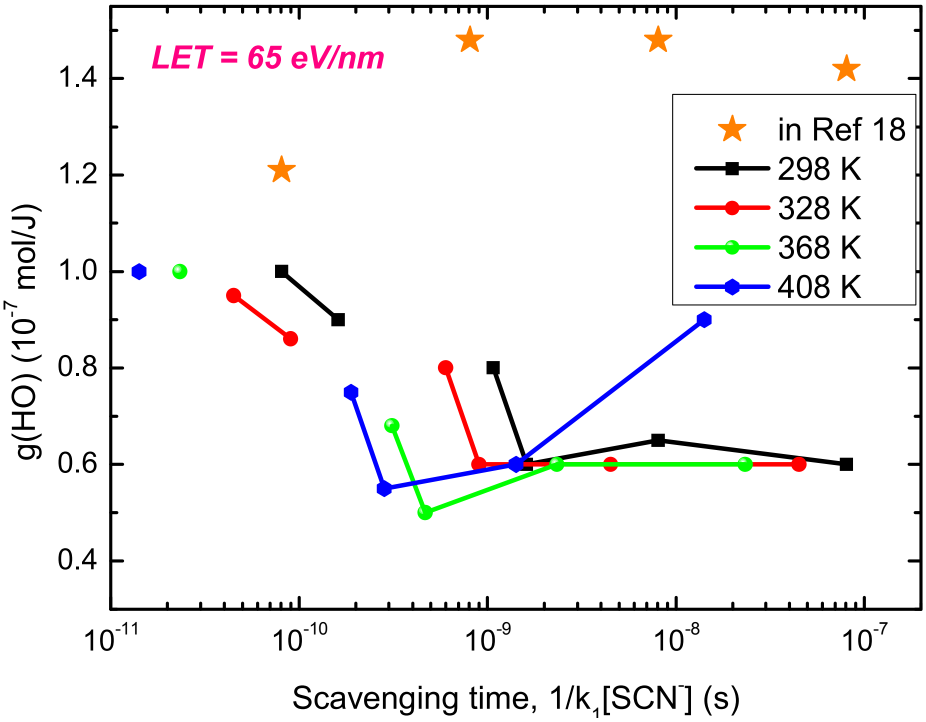

Figure 7. Radiolytic yield of $HO^{\bullet}$ as a function of scavenging time at 298, 328, 368 and 408 K for irradiation with O^{8+} ions having 65 eV/nm of LET. Shortest times corresponding to the scavenger concentrations of 0.5 and 1 M are disconnected from the other data because of the non-applicability of the Debye-Hückel ionic strength correction. Data from reference 18 are given at ambient temperature.

At earliest time, $HO^{\bullet}$-yields seems to be greater and greater. Unlike Ar^{18+} kinetics, this increase occurs in the range 2×10^{-10} to 2×10^{-9}s which is shifted of about -8×10^{-9}s compared to the yield increase under Ar^{18+}. Within this time range, non-homogeneous chemistry occurs. These fast decays should be therefore related to the yield and reactivity of $HO^{\bullet}$ escaped from the ionization tracks (track core) and/or $HO^{\bullet}$ formed in the penumbra (using the terminology of Magee and Chatterjee[27]).

In both irradiation cases, temperature accelerates the decay in the non-homogeneous time range that means the reactivity (its recombination) of $HO^{\bullet}$ is activated by temperature. In competition with the diffusion effect, it seems that temperature activation of $HO^{\bullet}$ recombination won. For denser tracks (expected with Ar^{18+}) $HO^{\bullet}$ cannot diffuse faster than $HO^{\bullet}$ that escape from less dense tracks (expected with O^{8+}). To explain the more efficient reactivity of $HO^{\bullet}$ in the neighborhood of Ar^{18+} tracks than in O^{8+} ones, a relevant part of the yield of initial $HO^{\bullet}$ formed during ionization by Ar^{18+} must come from energetic electrons which are ejected from the core track (δ-rays). These electrons are known to form the penumbra[27]. This zone has characteristics of low LET radiations. In this case $HO^{\bullet}$ can recombine in the spur in a few nanoseconds. That was recently shown by Monte Carlo simulation.[14,16] Radius of spurs does not expand too much with temperature (above 150°C) but the lifetime of the spurs decays from about 200 ns at ambient temperature to 50 ns at 150°C.[16] In the diffusion model, the local spurs let progressively the place to the homogeneous chemistry where escaped $HO^{\bullet}$ can react classically. Monte Carlo simulation could explain this behavior by identifying the reactions of interest but we have not found any simulation with high enough energy of ions. Unfortunately most of them are limited to about 30 eV/nm.[71,72]

At the highest ionic strengths (0.5 and 1 M), corresponding to the highest scavenging capacities and finally to the earliest accessible times, $HO^{\bullet}$-yield determinations seem more hypothetic. Many effects may occur in this domain: 1/ Concentrations of solute are in the order of magnitude of that of water which means generally that direct ionization of solute becomes probable. The mechanism then becomes too complex for classical calculation. 2/ Interference between the scavenging mechanism and the radiolysis of water in dense tracks may occur. As it is said above this proposition was done to explain a similar behavior published few years ago.[56] 3/ The ionic strength correction was applied to the rate constants, but it is not yet available for too high ionic strength.

Conclusion

This study has presented the first results on the effect of temperature on the track segment yield of $HO^\bullet$ under high LET irradiations. The results were obtained by combining three methods: pulse radiolysis with energetic heavy ions, scavenging method with thiocyanate and the temperature control of the solution with a flow cell especially developed for heavy ion irradiation.

The results were obtained for two different energetic ions, Ar^{18+} and O^{8+}, having LET in solution of 350 and 65 eV/nm. The kinetics of formation and decay of $(SCN)_2^{\bullet-}$ were recorded at various temperatures in the domain of 298-450 K and for various concentrations of SCN^- in order to scavenge $HO^\bullet$ species in the time range of 10^{-10}-10^{-7} s. The kinetics plots have been adjusted with a theoretical plot obtained by simulation of the SCN^- scavenging mechanism. This was done by taking care of correction of the rate constants by Arrhenius law and the ionic strength.

For both ions, a fast decay of the $HO^\bullet$-yield is observed in the nanosecond domain. The kinetics is flat around 100 ns. Around the ns time range, $HO^\bullet$-yields decay faster in the case of O^{+8} of 65 eV/nm than those do in case of Ar^{18+} of 350 eV/nm. In both cases, temperature accelerates the decays. Nevertheless the yields reach the same plateau at 100 ns: 0.4×10^{-7} mol/J at 350 eV/nm and 0.6×10^{-7} mol/J at 65 eV/nm. It was mainly discussed the differences of decays result from the structure of the track that would exhibit a domain of low LET (penumbra) in the case of Ar^{18+} ions.

For reason of lack of experimental data, there is no simulation for these high LET irradiations of water at high temperature yet. As this $HO^\bullet$ formation and decay is observed for the first time with high LET radiation, it should be interesting to study in details with Monte Carlo simulations the influence of the track structure on the reactivity of $HO^{\bullet}$ and also to exhibit which reaction(s) is activated in the non-homogeneous domain of the kinetics.

Many domains of chemical physics and biochemistry that are governed by non-homogeneous processes could be interested by such study. The structure of the energy deposition of energetic heavy ions looks like the intrinsic volume constraint we could obtain in a solid cylinder. And the effects are similar in terms of radical recombination and molecular production.[47,73-75] Any multi-phases systems, systems with interfaces or mesoporous media which can constrain the reactivity inside small volumes could be addressed with this angle of view. Actually combining effect of concentration and temperature effect is more identified as extreme conditions in radiation chemistry but not only. Various conditions of temperature exist in industry and in nature. Nuclear industry is targeted first for the water reactor chemistry but also for recycling or depository conditions of spent nuclear fuel.[76] Biochemistry where reactive oxygen species (typically radical species) are naturally involved is concerned especially for understanding why life exists in hydrothermal sources, in highly salts concentrated environments or in extraterrestrial highly irradiated environments under bombardment of heavy energetic particles. These extreme conditions could hypothetically play a role in the so-called “prebiotic chemistry”. This topic generated an abundant literature these last 10 years.[77,78]

AUTHOR INFORMATION

Corresponding Author

*G.B.: gerard.baldacchino@cea.fr

ACKNOWLEDGMENT

The authors would like to acknowledge GANIL staff for their help.

REFERENCES

1. G. V. Buxton, C. L. Greenstock, W. P. Helman and A. B. Ross, *Journal of Physical and Chemical Reference Data*, 1988, **17**, 513-886.
2. A. O. Allen, *The Radiation Chemistry of Water and Aqueous Solutions.*, D. Van Nostrand, Princeton, NJ, 1961.
3. T. Douky and J. Cadet, in *Radiation Chemistry. From Basics to Applications in Material and Life Sciences*, eds. M. Spotheim-Maurizot, M. Mostafavi, T. Douky and J. Belloni, EDP Sciences, 2008, pp. 177-190.
4. L. Bobyk, M. Edouard, P. Deman, M. Vautrin, K. Pernet-Gallay, J. Delaroche, J.-F. Adam, F. Esteve, J.-L. Ravanat and H. Elleaume, *Nanomedicine-Nanotechnology Biology and Medicine*, 2013, **9**, 1089-1097.
5. C. Sicard-Roselli, E. Brun, M. Gilles, G. Baldacchino, C. Kelsey, H. McQuaid, C. Polin, N. Wardlow and F. Currell, *Small (Weinheim an der Bergstrasse, Germany)*, 2014, **10**, 3338-3346.
6. J. W. T. Spinks and R. J. Woods, *An Introduction to Radiation Chemitry*, 3rd edn., John Wiley - Interscience, New York, 1990.
7. A. J. Elliot, M. P. Chenier, D. C. Ouellette and V. T. Koslowsky, *Journal of Physical Chemistry*, 1996, **100**, 9014-9020.
8. A. J. Elliot and D. M. Bartels, *The Reaction Set, Rate Constants and g-Values for the Simulation of the Radiolysis of Light Water over the Range 20° to 350°C Based on Information Available in 2008.* AECL-153-127160-450-001, AECL, 2009.
9. J. Takagi, J. M. Mincher, M. Yamaguchi and Y. Katsumura, in *Charged Particle and Photon Interactions with Matter. Recent Advances, Applications, and Interfaces.*, eds. Y. Hatano, Y. Katsumura and A. Mozumder, CRC Press, Taylor and Francis Group, Boca Raton, 2011, pp. 959-1023.
10. M. Lin and Y. Katsumura, in *Charged Particle and Photon Interactions with Matter. Recent Advances, Applications, and Interfaces.*, eds. Y. Hatano, Y. Katsumura and A. Mozumder, CRC Press, Taylor and Francis Group, Boca Raton, 2011, pp. 401-424.
11. A. J. Elliot, *Rate Constants and G-Values for the Simulation of the Radiolysis of Light Water over the Range 0–300°C.* , Atomic Energy of Canada Ltd., Chalk River, Ontario, 1994.
12. J. Meesungnoen, J. P. Jay-Gerin, A. Filali-Mouhim and S. Mankhetkorn, *Chemical Physics Letters*, 2001, **335**, 458-464.
13. J. Meesungnoen, J. P. Jay-Gerin, A. Filali-Mouhim and S. Mankhetkorn, *Canadian Journal of Chemistry-Revue Canadienne De Chimie*, 2002, **80**, 767-773.
14. S. Sanguanmith, Y. Muroya, J. Meesungnoen, M. Lin, Y. Katsumura, L. M. Kohan, D. A. Guzonas, C. R. Stuart and J. P. Jay-Gerin, *Chemical Physics Letters*, 2011, **508**, 224-230.
15. S. Sanguanmith, Y. Muroya, T. Tippayamontri, J. Meesungnoen, M. Lin, Y. Katsumura and J.-P. Jay-Gerin, *Physical Chemistry Chemical Physics*, 2011, **13**, 10690-10698.
16. S. Sanguanmith, J. Meesungnoen, Y. Muroya, M. Z. Lin, Y. Katsumura and J. P. Jay-Gerin, *Physical Chemistry Chemical Physics*, 2012, **14**, 16731-16736.
17. S. Sanguanmith, J. Meesungnoen and J.-P. Jay-Gerin, *Chemical Physics Letters*, 2013, **588**, 82-86.
18. D. Swiatla-Wojcik and G. V. Buxton, *Physical Chemistry Chemical Physics*, 2000, **2**, 5771-5771.

19. D. Swiatla-Wojcik and G. V. Buxton, *Physical Chemistry Chemical Physics*, 2000, **2**, 5113-5119.
20. D. Swiatla-Wojcik and G. V. Buxton, *Radiation Physics and Chemistry*, 2005, **74**, 210-219.
21. D. M. Bartels, *Radiation Physics and Chemistry*, 2009, **78**, 191-194.
22. D. Swiatla-Wojcik and G. V. Buxton, *Radiation Physics and Chemistry*, 2010, **79**, 52-56.
23. C. D. Alcorn, J. C. Brodovitch, P. W. Percival, M. Smith and K. Ghandi, *Chemical Physics*, 2014, **435**, 29-39.
24. S. Yamashita, M. Taguchi, G. Baldacchino and Y. Katsumura, in *Charged Particle and Photon Interactions with Matter. Recent Advances, Applications, and Interfaces.*, eds. Y. Hatano, Y. Katsumura and A. Mozumder, CRC Press, Taylor and Francis Group, Boca Raton, 2011, pp. 325-354.
25. G. Baldacchino and Y. Katsumura, in *Recent Trends in Radiation Chemistry*, eds. B. S. M. Rao and J. F. Wishart, World Scientific Publishing Co. Pte. Ltd., Singapore, 2010, pp. 231-254.
26. J. Laverne, in *Charged Particle and Photon Interactions with Matter. Chemical, Physicochemical, and Biological Consequences with Applications*, eds. A. Mozumder and Y. Hatano, Marcel Dekker, Inc., New York, Basel, 2004, pp. 403-429.
27. J. L. Magee and A. Chatterjee, in *Radiation Chemistry - Principles and Applications*, eds. J. Farhataziz and M. A. J. Rodgers, VCH Publishers, New York, 1987.
28. G. Baldacchino, G. Vigneron, J. P. Renault, S. Pin, S. Remita, Z. Abedinzadeh, S. Deycard, E. Balanzat, S. Bouffard, M. Gardes-Albert, B. Hickel and J. C. Mialocq, *Nuclear Instruments & Methods in Physics Research - Section B: Beam Interaction with Materials and Atoms*, 2003, **209**, 219-223.
29. G. Baldacchino, G. Vigneron, J. P. Renault, S. Pin, Z. Abedinzadeh, S. Deycard, E. Balanzat, S. Bouffard, M. Gardes-Albert, B. Hickel and J. C. Mialocq, *Chemical Physics Letters*, 2004, **385**, 66-71.
30. G. Baldacchino, G. Vigneron, J. P. Renault, S. Le Caer, S. Pin, J. C. Mialocq, E. Balanzat and S. Bouffard, *Nuclear Instruments & Methods in Physics Research - Section B: Beam Interaction with Materials and Atoms*, 2006, 288-291.
31. G. Baldacchino, *Radiation Physics and Chemistry*, 2008, **77**, 1218-1223.
32. G. Baldacchino, T. Maeyama, S. Yamashita, M. Taguchi, A. Kimura, Y. Katsumura and T. Murakami, *Chemical Physics Letters*, 2009, **468**, 275-279.
33. H. Christensen and K. Sehested, *Radiation Physics and Chemistry*, 1981, **18**, 723-731.
34. K. Haygarth, D. Janik, I. Janik and D. M. Bartels, *Journal of Physical Chemistry A*, 2010, **114**, 5034-5034.
35. K. Haygarth and D. M. Bartels, *Journal of Physical Chemistry A*, 2010, **114**, 7479-7484.
36. J. A. LaVerne, *Radiation Research*, 2000, **153**, 487-496.
37. K. Takahashi, J. A. Cline, D. M. Bartels and C. D. Jonah, *Review of Scientific Instruments*, 2000, **71**, 3345-3350.
38. G. Z. Wu, Y. Katsumura, Y. Muroya, X. F. Li and Y. Terada, in *International Symposium on Prospects for Application of Radiation toward the 21st Century*, eds. M. Washio, Y. Katsumura and N. Getoff, Radiation Physics and Chemistry, Waseda University, Tokyo, Japan, 2001, vol. 60, pp. 395-398.

39. G. Baldacchino, V. De Waele, H. Monard, S. Sorgues, F. Gobert, J. P. Larbre, G. Vigneron, J. L. Marignier, S. Pommeret and M. Mostafavi, *Chemical Physics Letters*, 2006, **424**, 77-81.
40. G. L. Hug, *Optical Spectra of Nonmetallic Inorganic Transient Species in Aqueous Solution*, U.S. Dept. of Commerce / National Bureau of Standard, 1981.
41. S. M. Pimblott and J. A. Laverne, *Journal of Physical Chemistry*, 1992, **96**, 746-752.
42. M. Chin and P. H. Wine, *Journal of Photochemistry and Photobiology a-Chemistry*, 1992, **69**, 17-25.
43. B. H. Milosavljevic and J. A. Laverne, *Journal of Physical Chemistry A*, 2005, **109**, 165-168.
44. G. V. Buxton and C. R. Stuart, *Journal of the Chemical Society-Faraday Transactions*, 1995, **91**, 279-281.
45. A. J. Elliot and F. C. Sopchyshyn, *International Journal of Chemical Kinetics*, 1984, **16**, 1247-1256.
46. G. Z. Wu, Y. Katsumura, Y. Muroya, M. Z. Lin and T. Morioka, *Journal of Physical Chemistry A*, 2001, **105**, 4933-4939.
47. S. Foley, P. Rotureau, S. Pin, G. Baldacchino, J. P. Renault and J. C. Mialocq, *Angewandte Chemie-International Edition*, 2005, **44**, 110-112.
48. S. Yamashita, G. Baldacchino, T. Maeyama, M. Taguchi, Y. Muroya, M. Z. Lin, A. Kimura, T. Murakami and Y. Katsumura, *Free Radic. Res.*, 2012, **46**, 861-871.
49. T. Maeyama, S. Yamashita, M. Taguchi, G. Baldacchino, L. Sihver, T. Murakami and Y. Katsumura, *Radiation Physics and Chemistry*, 2011, **80**, 1352-1357.
50. T. Maeyama, S. Yamashita, G. Baldacchino, M. Taguchi, A. Kimura, T. Murakami and Y. Katsumura, *Radiation Physics and Chemistry*, 2011, **80**, 535-539.
51. J. Bonin, I. Janik, D. Janik and D. M. Bartels, *Journal of Physical Chemistry A*, 2007, **111**, 1869-1878.
52. M. Taguchi, A. Kimura, R. Watanabe and K. Hirota, *Radiation Research*, 2009, **171**, 254-263.
53. M. Taguchi and T. Kojima, *Radiation Research*, 2005, **163**, 455-461.
54. J. A. Laverne, *Journal of Physical Chemistry*, 1988, **92**, 2808-2809.
55. J. A. LaVerne, *Radiation Research*, 1989, **118**, 201-210.
56. N. Chitose, Y. Katsumura, M. Domae, Z. L. Cai, Y. Muroya, T. Murakami and J. A. LaVerne, *Journal of Physical Chemistry A*, 2001, **105**, 4902-4907.
57. J. F. Ziegler, M. D. Ziegler and J. P. Biersack, *Nuclear Instruments & Methods in Physics Research Section B-Beam Interactions with Materials and Atoms*, 2010, **268**, 1818-1823.
58. C. Bataille, G. Baldacchino, R. P. Cosson, M. Coppo, C. Trehen, G. Vigneron, J. P. Renault and S. Pin, *Biochimica Et Biophysica Acta-General Subjects*, 2005, **1724**, 432-439.
59. J. A. Laverne and S. M. Pimblott, *Journal of Physical Chemistry*, 1991, **95**, 3196-3206.
60. P. Kirkegaard, E. Bjergbakke and J. V. Olsen, *Chemsimul: A chemical kinetics software package*, National Laboratory for Sustainable Energy, Riso DTU, December 2008.
61. M. Destriau, in *Cinétique et Dynamique Chimiques*, eds. M. Destriau, G. Dorthe and R. Ben-Aïm, Editions Technip, Paris, 1981, pp. 32-44.
62. J. H. Baxendale, P. L. T. Bevan and D. A. Stott, *Transactions of the Faraday Society*, 1968, **64**, 2389-2397.

63. D. Behar, P. L. T. Bevan and G. Scholes, *Journal of Physical Chemistry*, 1972, **76**, 1537-1542.
64. V. Nagarajan and R. W. Fessenden, *Journal of Physical Chemistry*, 1985, **89**, 2330-2335.
65. R. E. Weston and H. A. Schwarz, in *Chemical kinetics*, Prentice-Hall, Englewood Cliffs, N.J., 1972, pp. 165-171.
66. M. Destriau, in *Cinétique et Dynamique Chimiques*, eds. M. Destriau, G. Dorthe and R. Ben-Aïm, Editions Technip, Paris, 1981, pp. 76-80.
67. K. J. Laidler, in *Chemical Kinetics*, ed. K. J. Laidler, McGraw-Hill, London, 2nd Edition, International Student Edition edn., 1965, pp. 198-255.
68. G. V. Buxton and S. R. Mackenzie, *Journal of the Chemical Society-Faraday Transactions*, 1992, **88**, 2833-2836.
69. A. J. Elliot, D. R. McCracken, G. V. Buxton and N. D. Wood, *Journal of the Chemical Society-Faraday Transactions*, 1990, **86**, 1539-1547.
70. R. E. Weston and H. A. Schwarz, Prentice-Hall, Englewood Cliffs, N.J., 1972.
71. V. Cobut, Y. Frongillo, J. P. Patau, T. Goulet, M. J. Fraser and J. P. Jay-Gerin, *Radiation Physics and Chemistry*, 1998, **51**, 229-243.
72. Y. Frongillo, T. Goulet, M. J. Fraser, V. Cobut, J. P. Patau and J. P. Jay-Gerin, *Radiation Physics and Chemistry*, 1998, **51**, 245-254.
73. O. Roth, B. Dahlgren and J. A. LaVerne, *Journal of Physical Chemistry C*, 2012, **116**, 17619-17624.
74. J. Laverne, in *Charged Particle and Photon Interactions with Matter. Recent Advances, Applications, and Interfaces.*, eds. Y. Hatano, Y. Katsumura and A. Mozumder, CRC Press, Taylor and Francis Group, Boca Raton, 2011, pp. 425-444.
75. R. Musat, M. S. Alam and J. P. Renault, in *Recent Trends in Radiation Chemistry*, eds. J. F. Wishart and B. S. M. Rao, World Scientific, Singapore, 2010, pp. 325-346.
76. G. Baldacchino and B. Hickel, in *Radiation Chemistry. From Basics to Applications in Material and Life Sciences*, eds. M. Spotheim-Maurizot, M. Mostafavi, T. Douky and J. Belloni, EDP Sciences, 2008, pp. 53-64.
77. K. Takai, T. Gamo, U. Tsunogai, N. Nakayama, H. Hirayama, K. H. Nealson and K. Horikoshi, *Extremophiles*, 2004, **8**, 269-282.
78. M. J. Russell, L. M. Barge, R. Bhartia, D. Bocanegra, P. J. Bracher, E. Branscomb, R. Kidd, S. McGlynn, D. H. Meier, W. Nitschke, T. Shibuya, S. Vance, L. White and I. Kanik, *Astrobiology*, 2014, **14**, 308-343.